

Title	A computational and experimental study to determine a temporal issue in voluntary movement
Author(s)	李, 龍川
Citation	
Issue Date	2016-03
Type	Thesis or Dissertation
Text version	author
URL	<a href="http://hdl.handle.net/10119/13645">http://hdl.handle.net/10119/13645</a>
Rights	
Description	Supervisor: Tanaka Hirokazu, 情報科学研究科, 修士

# **A computational and experimental study to determine a temporal issue in voluntary movement**

By Longchuan Li

A thesis submitted to  
School of Information Science,  
Japan Advanced Institute of Science and Technology,  
in partial fulfillment of the requirements  
for the degree of  
Master of Information Science  
Graduate Program in Information Science

Written under the direction of  
Associate Professor Hirokazu Tanaka

March, 2016

# A computational and experimental study to determine a temporal issue in voluntary movement

By Longchuan Li (1310212)

A thesis submitted to  
School of Information Science,  
Japan Advanced Institute of Science and Technology,  
in partial fulfillment of the requirements  
for the degree of  
Master of Information Science  
Graduate Program in Information Science

Written under the direction of  
Associate Professor Hirokazu Tanaka

and approved by  
Associate Professor Hirokazu Tanaka  
Professor Jianwu Dang  
Professor Masato Akagi

February, 2016 (Submitted)

# Contents

<b>1</b>	<b>Introduction</b>	<b>4</b>
<b>2</b>	<b>Research Background</b>	<b>6</b>
2.1	A general framework of goal directed behavior . . . . .	6
2.1.1	Optimal feedback control . . . . .	7
2.2	finite- and infinite-horizon . . . . .	7
2.2.1	Fitt's law . . . . .	7
2.3	finite- and infinite-horizon optimal feedback control . . . . .	8
2.3.1	finite-horizon optimal feedback control . . . . .	8
2.3.2	infinite-horizon optimal feedback control . . . . .	10
<b>3</b>	<b>Method</b>	<b>11</b>
3.1	Movement with external perturbations . . . . .	11
3.2	Time-variant and -invariant gains . . . . .	11
<b>4</b>	<b>Experiment conduct</b>	<b>14</b>
4.1	visually guided target reaching task with external perturbations . . . . .	14
4.2	handedness compute . . . . .	16
<b>5</b>	<b>Simulations</b>	<b>21</b>
5.1	Simulations based on finite-horizon control model . . . . .	23
5.2	Simulations based on infinite-horizon control model . . . . .	24
5.3	Sensory delay . . . . .	24
<b>6</b>	<b>Data analysis</b>	<b>27</b>
6.1	Whole data analysis . . . . .	27
6.2	Separated data . . . . .	27
<b>7</b>	<b>Tuning parameters</b>	<b>32</b>
<b>8</b>	<b>Conclusion</b>	<b>37</b>
8.1	Summary . . . . .	37
8.2	Discussion . . . . .	37
8.3	Conclusion . . . . .	37
8.4	Acknowledgement . . . . .	38

# List of Figures

1.1	Problems brain faces during a voluntary movement . . . . .	5
2.1	Goal directed behavior . . . . .	7
2.2	finite- and infinite-horizon . . . . .	8
3.1	movement with external perturbations . . . . .	12
3.2	time-variant and -invariant gains . . . . .	12
4.1	Experiment design . . . . .	15
4.2	Perturbations . . . . .	16
4.3	Paradigm1 . . . . .	17
4.4	Paradigm2 . . . . .	18
4.5	Block . . . . .	19
5.1	Visual disturb corrections of finite horizon control . . . . .	23
5.2	Force disturb corrections of finite horizon control . . . . .	24
5.3	Visual disturb corrections of infinite horizon control . . . . .	25
5.4	Force disturb corrections of infinite horizon control . . . . .	26
6.1	Corrections against visual perturbations . . . . .	28
6.2	Corrections against force perturbations . . . . .	28
6.3	Separate data of visual condition . . . . .	29
6.4	Separate data of force condition . . . . .	30
7.1	Orders in visual condition . . . . .	34
7.2	Orders in force condition . . . . .	35
7.3	tune . . . . .	36

# List of Tables

4.1	Perturbation type . . . . .	15
4.2	Handedness compute . . . . .	20
6.1	Visual condition . . . . .	31
6.2	Force condition . . . . .	31

# Chapter 1

## Introduction

We live in space and time, and we are making movements all the time. When we are making a voluntary movement, brain is facing two questions: 1. How to decide the trajectory? 2. How to determine the duration? The first question is focus on space domain, and the second is focus on time domain. These problems are illustrated as the figure 1.1 .

To explaining experimentally observed properties of human movements, Optimal control theory was broadly applied and got many successes. Upper-limb movement, for example, exhibit a variety of invariant laws including spatially smooth trajectories and power laws between velocity and curvature. These characteristics have been modelled within the framework of optimal control theory, indicating that human movements are optimized with respect to certain objective functions. These researches had successfully discovered many computational principles of visually guided reaching in space domain. In contrast, little is investigated about how movement duration is determined in voluntary movements, despite the fact that movement duration exhibits stereotypical laws such as Fitts' law (the duration of a rapidly movement is a logarithmic function of the ratio between the movement distance and the target width) for reaching and the main sequence for eye saccade [1] [2] [3].

This study attempts to address how movement duration is determined in visually guided reaching. There are two model proposals. One is that the movement duration is determined before movement onset based on certain criterion and that movement is optimized over that finite duration (finite-horizon control) [4]. The other is that movement duration is not predetermined and that movement is optimized over infinite period (infinite-horizon control). In infinite horizon control, the movement duration is not a pre-planned parameter but emerges when movement is terminated [5]. Although whether movement is optimized over a finite or infinite period sounds a technical problem, it has an implication to a question of whether the brain predetermines a movement duration or not. Although both models can reproduce Fitts' law and the main sequence equally well, their model predictions have not been systematically investigated in an experimentally testable way. We therefore compared predictions of these models in detail and tested those predictions in a behavioral experiment.

In the Chapter 2, the background will be introduced. A general framework of goal

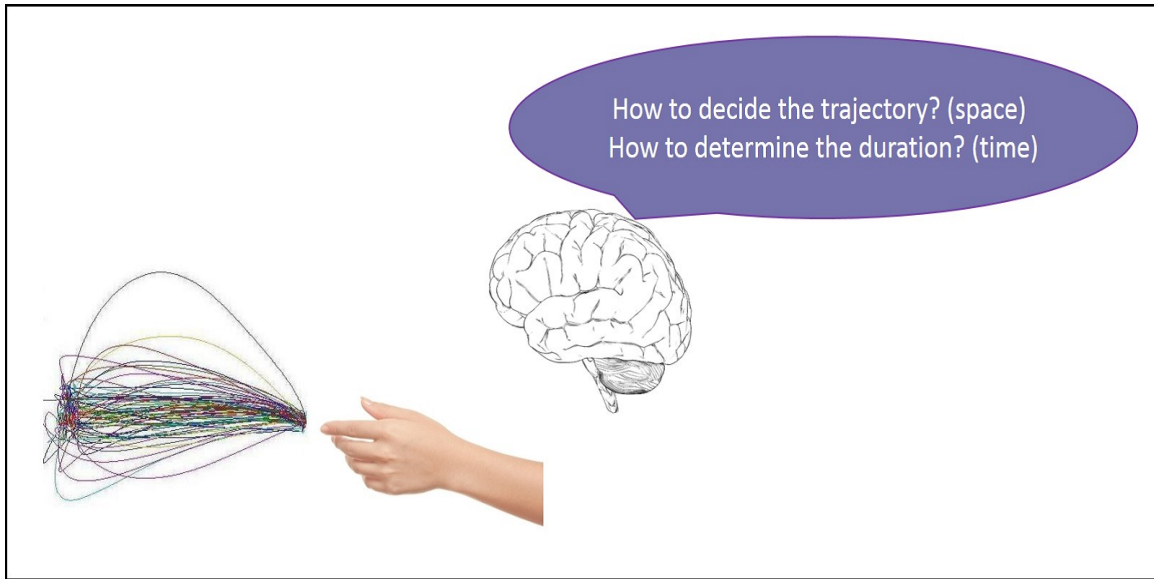


Figure 1.1: Problems brain faces during a voluntary movement

directed behavior will be briefly discussed, the concept of “finite-horizon” and “infinite-horizon” will be explained in examples, and the differences of these two theories will be discussed.

In the Chapter 3, the method for comparing these two models will be discussed.

In the Chapter 4, the behavioral experiment will be introduced base on the method.

In the Chapter 5, before demonstrating the experiment result, the numerical prediction will be provided through Matlab simulations.

In the Chapter 6, the experiment data will be analysed to compare with the simulations, in this chapter, we want to find out within which theory, the experiment result is better explained.

In the Chapter 7, numerical simulation will be further discussed because we found that different parameters may lead to different simulation results in finite-horizon control models.

In the Chapter 8, summaries, conclusions and discussions will be generated base on the results above.

# Chapter 2

## Research Background

### 2.1 A general framework of goal directed behavior

According to [6] , a general framework of goal directed behavior was illustrated as the figure 2.1 ,

When we have a goal(making a movement), the motor command generator generates motor commands  $u$  in order to achieve it. The motor commands change state  $x$  according to equation (2.1).

$$dx = Ax + Budt + \sum_{i=1}^q F_i x \beta_i + \sum_{j=1}^s R_j u \gamma_j + GdW \quad (2.1)$$

After a sensory delay, we got an observation of sensory consequences from our sensory system according to equation (2.2).

$$dy = Cx + Dd\xi \quad (2.2)$$

In another pathway, we have a prediction of the sensory consequences base on the forward model which contains our estimation of the state ( $\hat{x}$ ). So we learn the difference between the observation and prediction by Kalman filtering (2.3).

$$d\hat{x} = (A\hat{x} + Bu)dt + K(dy - C\hat{x}dt) \quad (2.3)$$

We change our believes and new motor command was generated until the goal is achieved (2.4).

$$u = -L\hat{x} \quad (2.4)$$

Where  $A, B, C, D, G, F_i, R_j$  are constant matrices,  $\beta_i, \gamma_j, \xi, W$  are independent wiener processes,  $K$  refers to Kalman filter gains matrix,  $L$  refers to control gains matrix,  $y$  is the observation of the state.

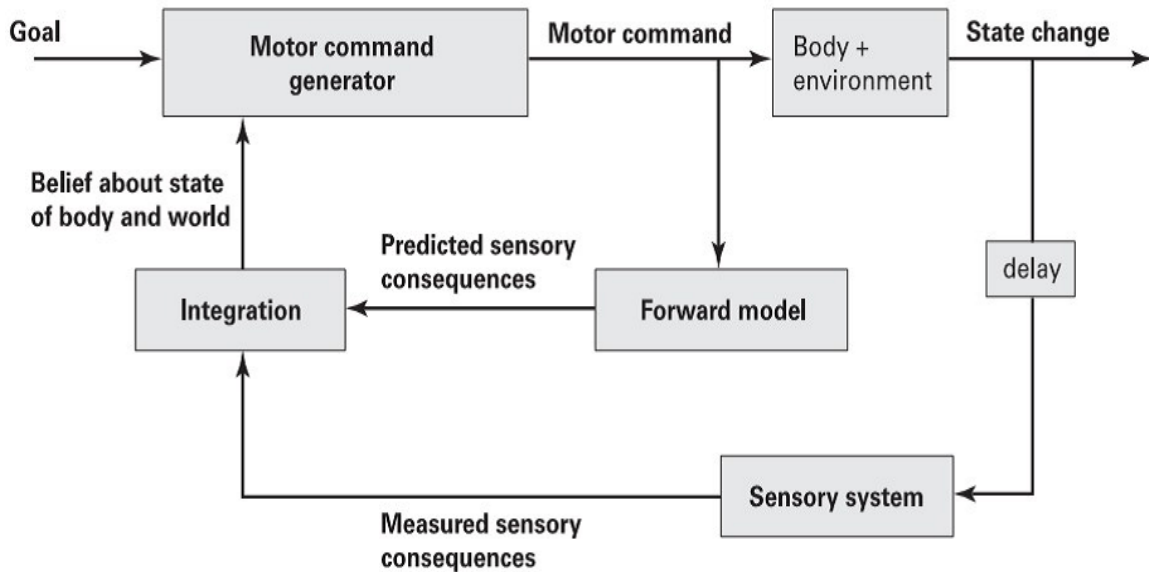


Figure 2.1: Goal directed behavior

### 2.1.1 Optimal feedback control

In order to achieve the goal above, we should devise a policy which species a series of actions that should be performed for each possible state. Ideally, the policy is a mapping from the state to the action. If we consider the task error and effort we should pay for achieving the goal as cost, optimal feedback control is to find the actions to minimize the totally future cost for each state, suppose we want to be as accuracy as we can and pay as less effort as we can.

## 2.2 finite- and infinite-horizon

The concepts finite- and infinite-horizon sounds difficult to understand, here I explain them by an example as figure 2.2 ,

If I want to use my hand to touch a big button, I can finish it in a very short period (finite-horizon), but if we consider an extremely condition, if I am aiming to use a certain point on my tip to touch a certain point on the button, I will achieve the goal in infinite time (infinite-horizon).

The mathematical principle can be proved by Fitts's law.

### 2.2.1 Fitt's law

Paul Fitts[7] have proposed a method to measure the difficulty of target reaching task based on information analogy in 1954. If we ignore the size of the tip, The duration of a target reaching task is proportional to the distance between hand and target, and is inversely proportional to the broad of the target as equation (2.5),

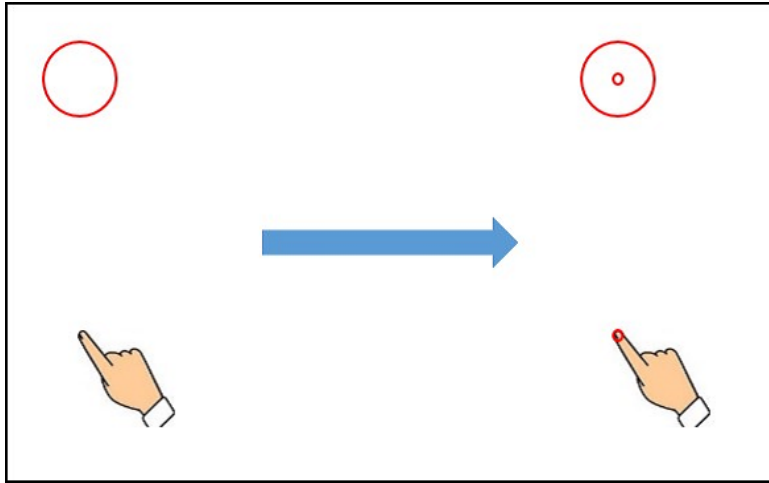


Figure 2.2: finite- and infinite-horizon

$$T = a + b \log_2 \left( 2 \frac{D_s}{W_t} \right) \quad (2.5)$$

where  $a$ ,  $b$  are coefficients,  $D_s$  refers to distance,  $W_t$  refers to width.

In our example, if  $W_t$  is a point (infinite small),  $T$  will be infinite large, and the movement duration will be infinite. So the key point is how much we can bare the task error (how much do we care about the accuracy).

## 2.3 finite- and infinite-horizon optimal feedback control

### 2.3.1 finite-horizon optimal feedback control

These two models are built by Todorov and Ning. Todorov's finite-horizon optimal feedback control model says that the movement duration is determined before movement onset based on certain criterion and movement is optimized over that finite duration. His model is defined in discrete form while Ning's in continuous form, For easy comparison, we use Phillis's definition. According to Phillis's paper [8], if we define the estimation error weight matrix as  $U$ , final error weight matrix as  $H$ , running error cost and motor cost as  $Q$  and  $R$ .

With Phillis's definitions,

$$\tilde{x} = x - \hat{x} \quad (2.6)$$

$$X \equiv \begin{bmatrix} x \\ \tilde{x} \end{bmatrix},$$

$$\begin{aligned}
d\bar{\omega} &\equiv \begin{bmatrix} d\omega \\ d\xi \end{bmatrix}, \\
\bar{A} &\equiv \begin{bmatrix} A - BL & BL \\ 0 & A - KC \end{bmatrix}, \\
\bar{F} &\equiv \begin{bmatrix} F & 0 \\ F & 0 \end{bmatrix}, \\
\bar{G} &\equiv \begin{bmatrix} G & 0 \\ G & -KD \end{bmatrix},
\end{aligned}$$

Then the system equations became:

$$dX = \bar{A}Xdt + \bar{F}Xd\beta + \bar{G}d\bar{\omega} \quad (2.7)$$

And Pillis further defined:

$$\begin{aligned}
\bar{Q} &\equiv \begin{bmatrix} Q + L^T RL & L^T RL \\ L^T RL & L^T RL \end{bmatrix}, \\
P &= \begin{bmatrix} P_{11} & P_{12} \\ P_{21} & P_{22} \end{bmatrix} = E(XX^T), \\
S &= \begin{bmatrix} S_{11} & 0 \\ 0 & S_{22} \end{bmatrix},
\end{aligned}$$

The optimal Gains K and L from  $t_0$  to  $t_f$  are determined by the following equations:

$$\dot{P} = \bar{A}P + P\bar{A}^T + \sum_{j=1}^s \bar{R}_j P \bar{R}_j^T + \bar{G}\bar{G}^T \quad (2.8)$$

$$\dot{S} = -(\bar{Q} + \bar{A}^T S + S\bar{A} + \sum_{j=1}^s \bar{R}_j^T S \bar{R}_j) \quad (2.9)$$

$$K = P_{22}C^T(DD^T)^{-1} \quad (2.10)$$

$$L = [R + \sum_{j=1}^s \bar{R}_j^T (S_{11} + S_{22}) \bar{R}_j]^{-1} B^T S_{11} \quad (2.11)$$

With boundary conditions  $F_{11}(t_f) = H$ ,  $F_{22}(t_f) = U$ ,  $P_{11}(0) = P_{22}(0) = E(x_0 x_0^T)$ ,

### 2.3.2 infinite-horizon optimal feedback control

Qian's infinite-horizon model says movement duration is not predetermined and that movement is optimized over infinite period. The difference in equations is:  $\dot{P}$  and  $\dot{S}$  are zeros. So the (2.8), (2.9) differential equations become identical equations. There is no boundary conditions and  $\bar{Q}$  became

$$\bar{Q} \equiv \begin{bmatrix} Q + L^T R L & L^T R L \\ L^T R L & L^T R L + U \end{bmatrix},$$

$H$  become zeros because there is no final error in infinite-horizon control, and there is no final accuracy cost. In this case,  $P, S$  can be extracted by Kronecker products.

# Chapter 3

## Method

### 3.1 Movement with external perturbations

The method to discriminate whether finite- or infinite-horizon control is used in goal directed movement is illustrated in figure 3.1 .

If we consider a movement in one dimension, the movement is only happened on that dimension, the state does not change anymore on other dimensions. If we extend the movement to two dimensions, while an external perturbation was added on the dimension which is orthogonal to the movement dimension, the state deviate from “zeros” on that dimension. In order to reach the target, a velocity should be generated to make corrections. If the external perturbations are added on different timings, we can compare the correction profile of different timings.

### 3.2 Time-variant and -invariant gains

In both of these two models, the gains are precomputed before making the movements, so it is supposed that the arm is using a same group of gains to direct the movement no matter whether there is a perturbation or not.

As described in chapter 2, the K, L gains in finite-horizon control is determined by differential equations(6),(7). In infinite- horizon control, differential equations(6),(7)become identities, and can be extracted by using Kronecker products. So the key difference between these two models are: K, L gains in finite-horizon control are time-variant, in infinite-horizon are time-invariant.

The K,L gains are indeed matrices, for easy comparison, we just pick up one scalar from gains matrices of each model. The time-variant and time-invariant gains can be illustrated as figure 3.2.

Despite the sensory delay, if the perturbation is realized at 0.2s, The arm make corrections from 0.2 to  $t_f$ , similarly, if the perturbation is realized at 0.4s, The arm make corrections from 0.4 to  $t_f$ . Because the movements(and corrections) are directed by the gains, if the gains are time-variant, these two corrections should be different, otherwise, if the gains are time-invariant and  $t_f = \infty$  , the movement corrections should be same.

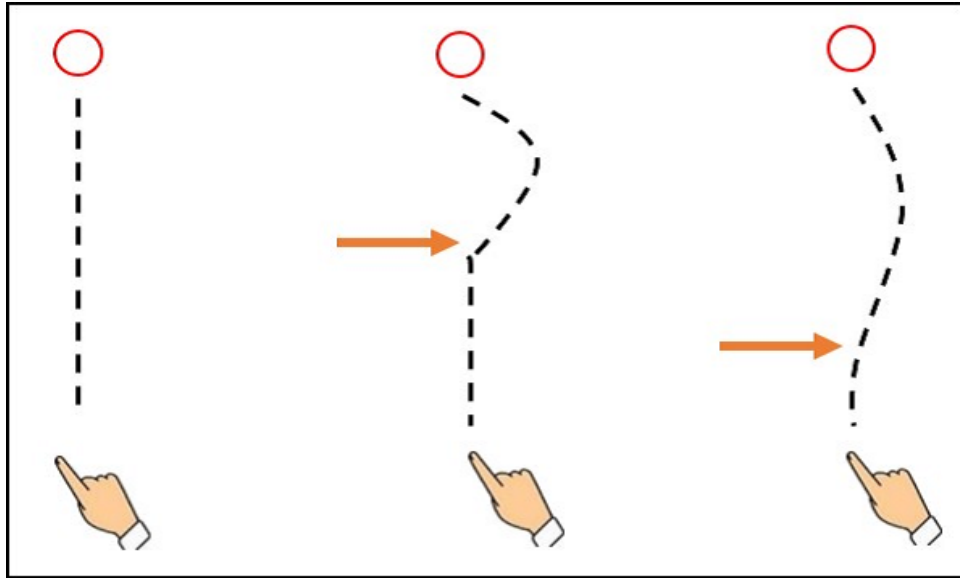


Figure 3.1: movement with external perturbations

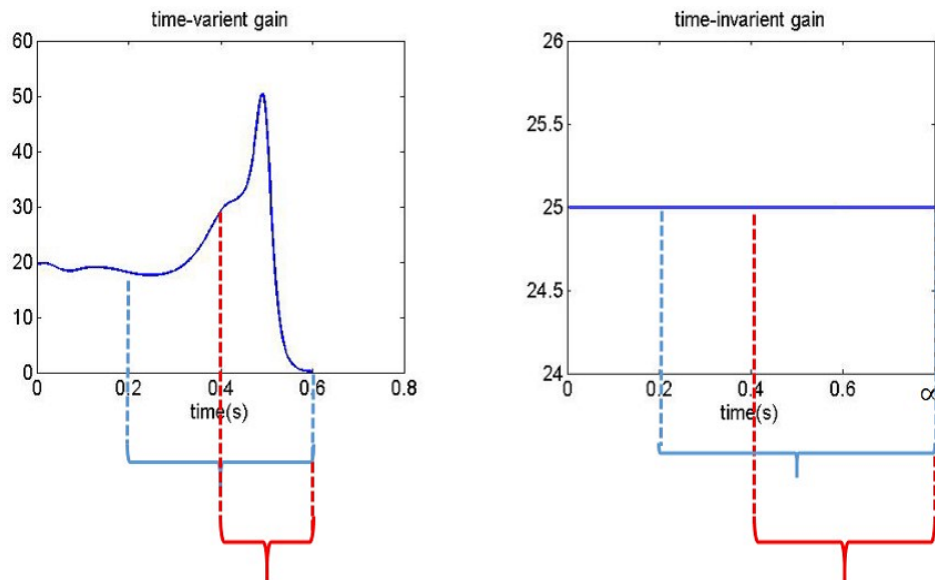


Figure 3.2: time-variant and -invariant gains

The reason is: if the gains are time-variant and  $t_f$  is a finite number, the gains from 0.2 to  $t_f$  and from 0.4 to  $t_f$  are different, if the gains are time-invariant and  $t_f$  is infinite, the gains from 0.2 to  $\infty$  and from 0.4 to  $\infty$  are same.

# Chapter 4

## Experiment conduct

### 4.1 visually guided target reaching task with external perturbations

Ten subjects participated in a point-to-point reaching task with or without perturbations as figure 4.1 . The hand movement is measured by a manipulandum. Above the manipulandum is a screen, and the positions of hand and target are shown on the screen. The movement amplitude is 20cm. To normalize subjects' movement pace, we asked them to finish a movement within 550ms~650ms in control trials and use the same pace in the perturbation trials. They are instructed to care more about time than accuracy.

Indeed, we provided two kinds of instructions in pilot experiment: 1. finish a movement within 550ms650ms. 2. finish a movement in a comfortable speed. But the word “comfortable” is ambiguous, everyone has different feeling, so the movement durations are so different. So we use the instructions above to normalize them in main experiment. Each subject performs seven sequences. Three sequences for normalization and four sequences for data analysis.

In some trials, there was no perturbation and the subjects made normal, control movements. In other trials, a visual perturbation (jump of cursor of 4 cm orthogonal to movement direction) or force perturbation (impulse of 10 N 50 ms orthogonal to movement direction) was imposed at early ( 100 ms ) ,middle ( 200 ms) or late ( 300 ms) timing as figure 4.1. Perturbation directions (i.e., left or right) were randomized on a trial basis to avoid any effect of adaptation or expectation. We measured the hand position and analyzed movement corrections against those perturbations.

They performed forward movements and backward movements equally in perturbation sequences. There are seven blocks for each subject. The experiment paradigms are shown as figure 4.3, 4.4. Five of the ten subjects performed as paradigm 1, other 5 subjects performed paradigm 2 equally.

The perturbation block is shown as Figure 4.5.

The perturbation types are shown as table 4.1.

Each perturbation block contains 140 trials: 20 trials without perturbations, 20 trials with early visual perturbations(100ms), 20 trials with middle visual perturbation-

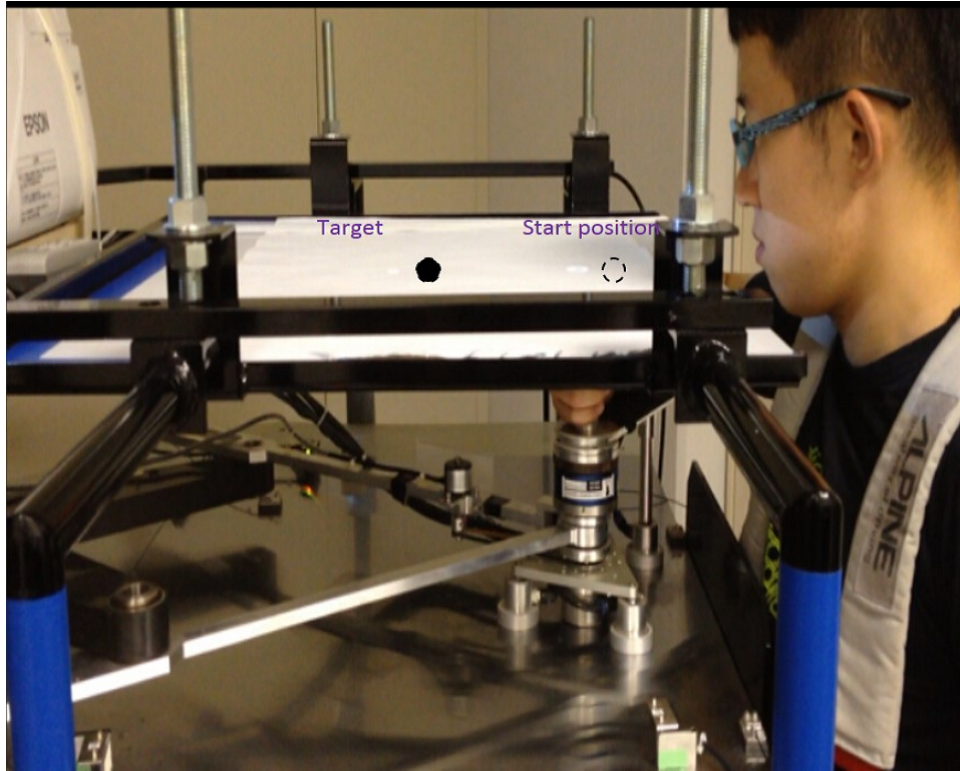


Figure 4.1: Experiment design

Table 4.1: Perturbation type

Force channel	×	×	→	←	×
Cursor displacement	×	→	×	×	←

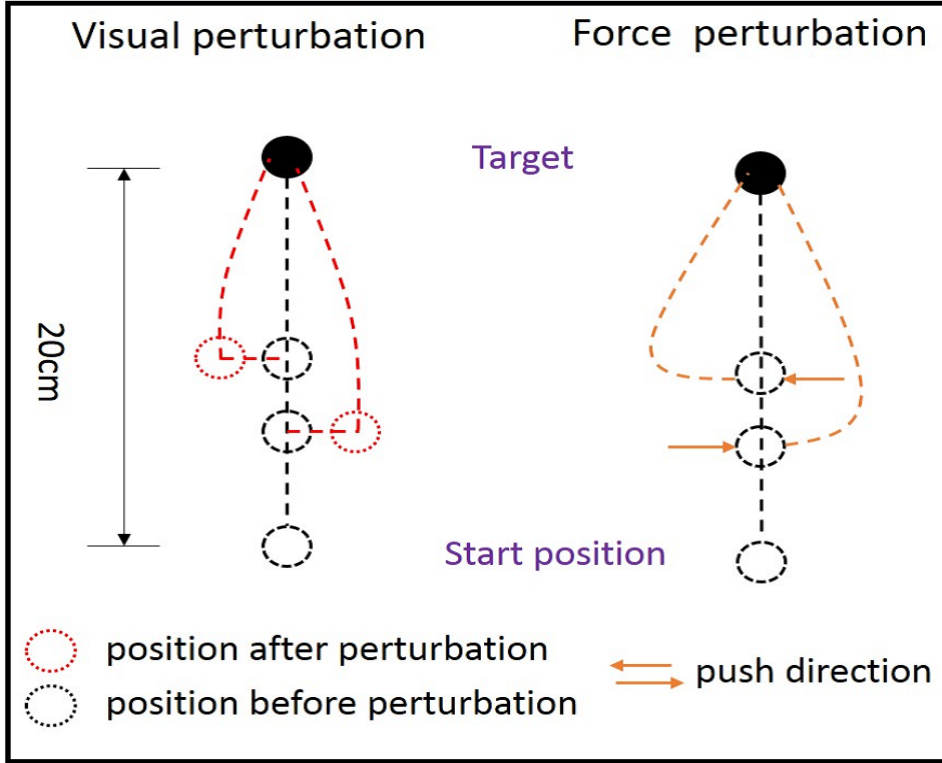


Figure 4.2: Perturbations

s(200ms), 20 trials with late visual perturbations(300ms), 20 trials with early force perturbations(100ms), 20 trials with middle force perturbations(200ms), 20 trials with late force perturbations(300ms).

## 4.2 handedness compute

All the subjects performed their task by right hand, so we computed their handedness according to their report and the equation below [9].

$$H = 100 \cdot \frac{\sum_{i=1}^n X(i, R) - \sum_{i=1}^n X(i, L)}{\sum_{i=1}^n X(i, R) + \sum_{i=1}^n X(i, L)} \quad (4.1)$$

The range of  $H$  is  $-100 \leq H \leq +100$ , if  $H > 0$ , that implies that the subject is right handed. So in our experiment, all of the ten subjects are right handed.

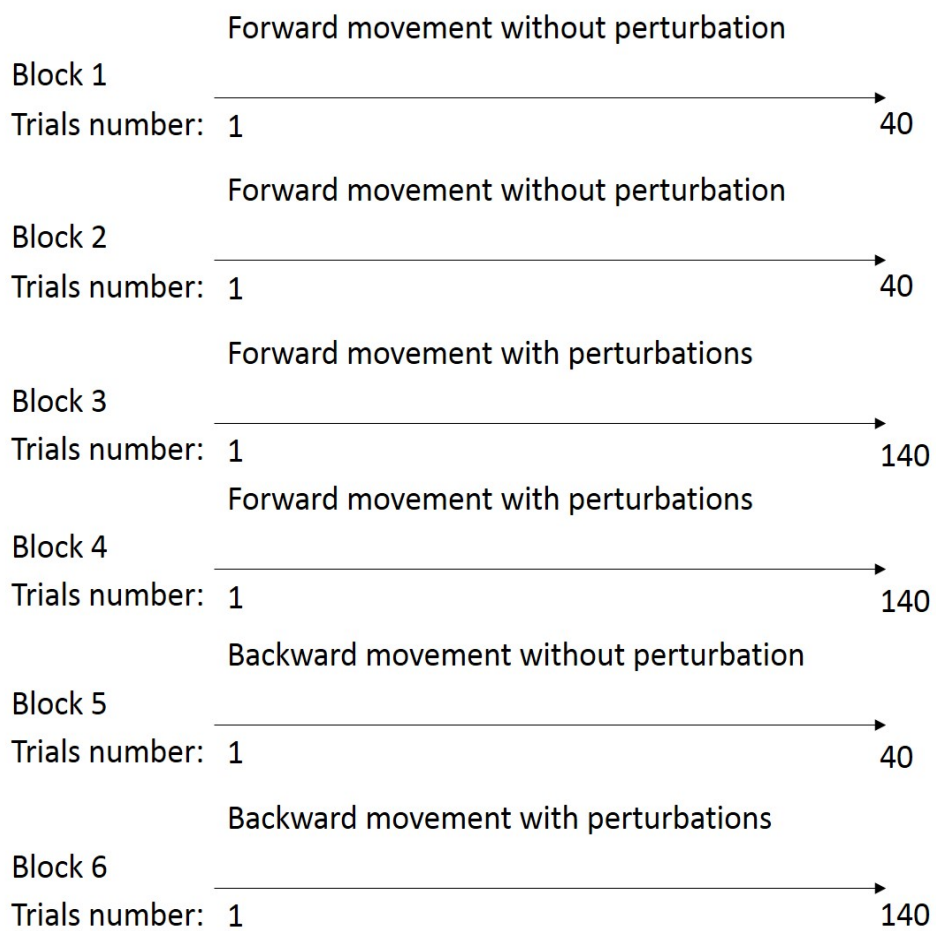


Figure 4.3: Paradigm1

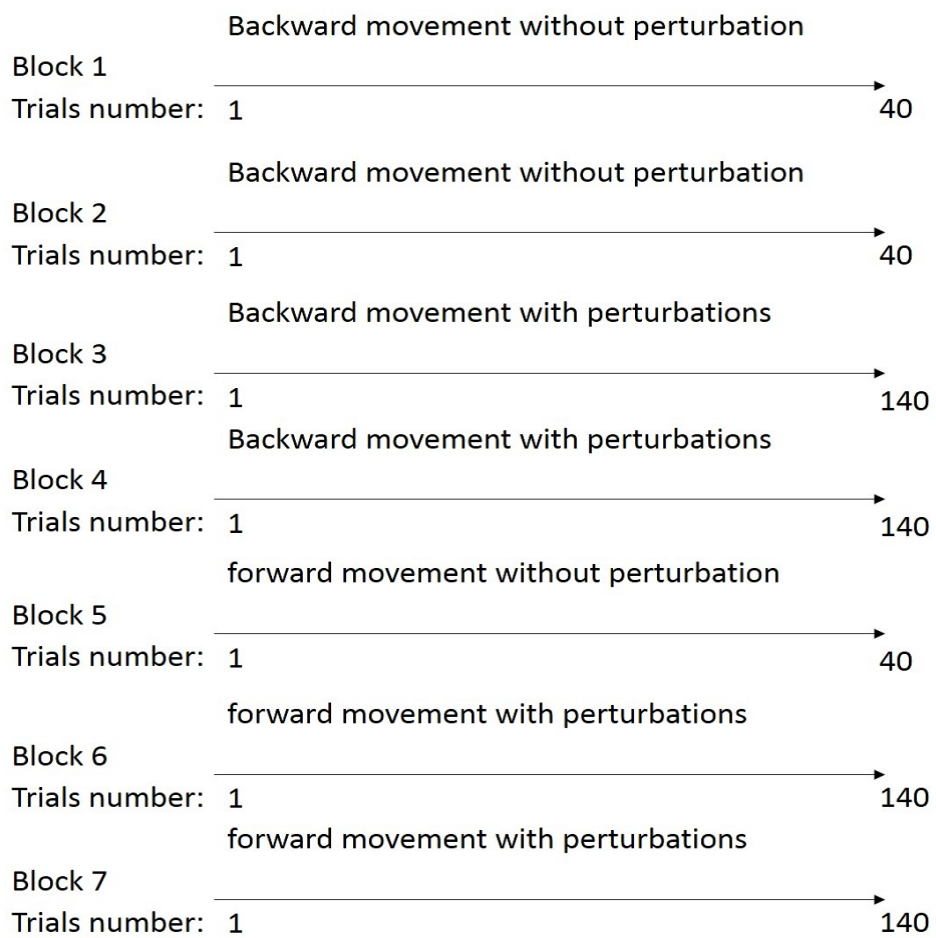


Figure 4.4: Paradigm2

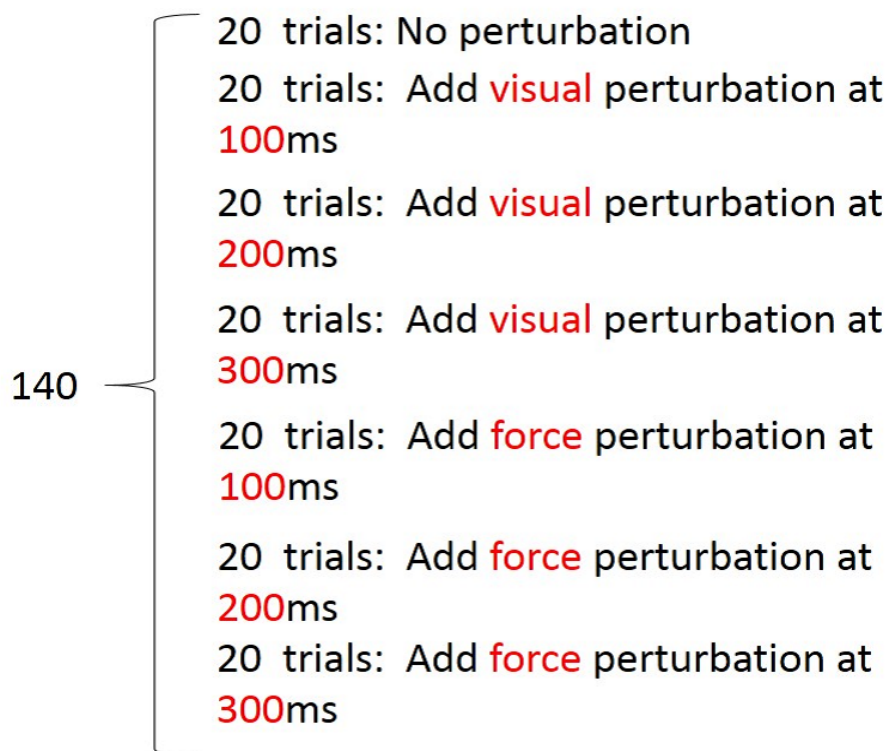


Figure 4.5: Block

Table 4.2: Handedness compute

Item \ Subject	E.S.	M.O.	H.A.	H.I.	Y.I.	K.I.	S.T.	K.S.	Y.U.	H.S.
Writing	R	R	R	R	R	R	R	R	R	R
Drawing	R	R	R	R	R	R	R	R	R	R
Throwing	R	R	R	R	R	R	R	R	R	R
Scissors	R	R	R	R	R	R	R	R	R	R
Toothbrush	R	LR	R	R	R	R	LR	R	R	R
Knife	R	R	R	R	R	R	R	R	R	R
Spoon	R	R	R	R	R	R	LR	R	R	R
Broom	LR	R	R	LR	R	L	L	R	R	LR
Striking match	R	R	R	R	R	R	R	R	R	R
Opening box	LR	R	R	R	R	R	LR	R	R	R
Kick	R	R	R	R	R	R	LR	R	R	R
Use one eye	R	R	R	R	R	L	LR	LR	LR	R
Handedness	83	92	100	92	100	67	42	92	92	92

# Chapter 5

## Simulations

Before taking a look at the experiment result, we made predictions by simulated this reaching experiment using the formulation of optimal feedback control proposed by Phillis [8], as Todorov's and Qian's formulations differ considerably and are difficult for a direct comparison, we chose the model parameters so as to be consistent with previous studies. The Kalman and feedback gains were precomputed so as to minimize the quadratic cost function over a finite period (finite-horizon control) or over an infinite period (infinite-horizon control). We then defined the movement correction as velocity profile in a control trial subtracted from one in a perturbation trial.

We modeled a single-joint target reaching movement with external perturbations. All the effect of the muscles is represented with the force  $f(t)$  acting on the hand. According to [10], the motor command  $u(t)$  transforms into force  $f(t)$  through a second-order muscle-like low-pass filter. To simplify the computation, here we use a first-order low-pass filter according to [12][13].

$$t_e \dot{f} + f = u \quad (5.1)$$

According to [13], the 2-D arm movement in the discrete form are:

$$f_x(t + \Delta t) = e^{-\Delta t/t_e} f_x(t) + u_x(t) + (u_x(t)\varepsilon_t^1 + u_y(t)\varepsilon_t^2)\sigma_u \quad (5.2)$$

$$f_y(t + \Delta t) = e^{-\Delta t/t_e} f_y(t) + u_y(t) + (u_y(t)\varepsilon_t^2 - u_x(t)\varepsilon_t^1)\sigma_u \quad (5.3)$$

In our simulation, we transformed the equations into continuous form:

$$\dot{f}_x = (-f_x + u_x)/t_e + (u_x\varepsilon_t^1 + u_y\varepsilon_t^2)\sigma_u \quad (5.4)$$

$$\dot{f}_y = (-f_y + u_y)/t_e + (u_y\varepsilon_t^2 - u_x\varepsilon_t^1)\sigma_u \quad (5.5)$$

The system has six state variables:

$$x = [p_x \quad p_y \quad v_x \quad v_y \quad a_x \quad a_y]^T,$$

where  $p_x, p_y$  represent the distances between target and the current hand position in  $x$  and  $y$  dimensions,  $v_x, v_y, a_x, a_y$  represent to the velocities and accelerations in those two dimensions. Refers to [4][5][11][13], we set:

$t_e = 0.04, m = 1$  (the hand is modeled as a point-mass).

$$A = \begin{bmatrix} 0 & 0 & 1 & 0 & 0 & 0 \\ 0 & 0 & 0 & 1 & 0 & 0 \\ 0 & 0 & 0 & 0 & 1/m & 0 \\ 0 & 0 & 0 & 0 & 0 & 1/m \\ 0 & 0 & 0 & 0 & -1/t_e & 0 \\ 0 & 0 & 0 & 0 & 0 & -1/t_e \end{bmatrix},$$

$$B = \begin{bmatrix} 0 & 0 \\ 0 & 0 \\ 0 & 0 \\ 0 & 0 \\ 1/t_e & 0 \\ 0 & 1/t_e \end{bmatrix},$$

$$C = \begin{bmatrix} 1 & 0 & 0 & 0 & 0 & 0 \\ 0 & 1 & 0 & 0 & 0 & 0 \\ 0 & 0 & 1 & 0 & 0 & 0 \\ 0 & 0 & 0 & 1 & 0 & 0 \\ 0 & 0 & 0 & 0 & 1 & 0 \\ 0 & 0 & 0 & 0 & 0 & 1 \end{bmatrix},$$

$$D = \begin{bmatrix} 0.001 & 0 & 0 & 0 & 0 & 0 \\ 0 & 0.001 & 0 & 0 & 0 & 0 \\ 0 & 0 & 0.01 & 0 & 0 & 0 \\ 0 & 0 & 0 & 0.01 & 0 & 0 \\ 0 & 0 & 0 & 0 & 0.05 & 0 \\ 0 & 0 & 0 & 0 & 0 & 0.05 \end{bmatrix},$$

$$F = 0.05B,$$

$$G = 0.005 \begin{bmatrix} 1 & 0 & 0 & 0 & 0 & 0 \\ 0 & 1 & 0 & 0 & 0 & 0 \\ 0 & 0 & 1 & 0 & 0 & 0 \\ 0 & 0 & 0 & 1 & 0 & 0 \\ 0 & 0 & 0 & 0 & 1 & 0 \\ 0 & 0 & 0 & 0 & 0 & 1 \end{bmatrix},$$

$$dt = 0.001,$$

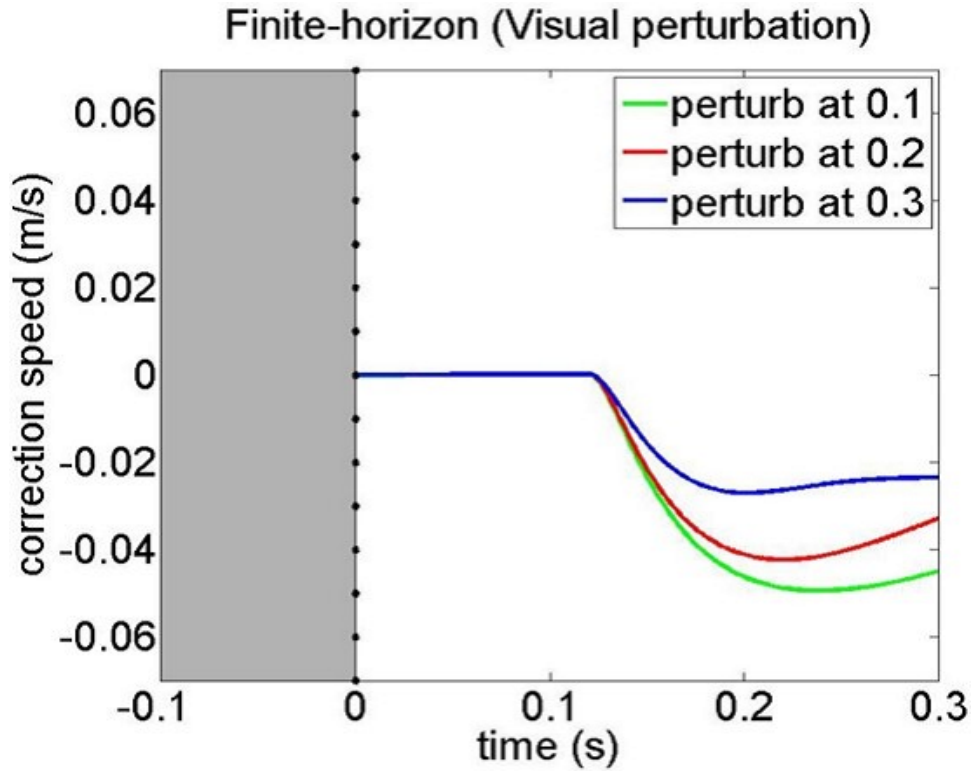


Figure 5.1: Visual disturb corrections of finite horizon control

$$Q=U=H= \begin{bmatrix} 1 & 0 & 0 & 0 & 0 & 0 \\ 0 & 1 & 0 & 0 & 0 & 0 \\ 0 & 0 & 0.1 & 0 & 0 & 0 \\ 0 & 0 & 0 & 0.1 & 0 & 0 \\ 0 & 0 & 0 & 0 & 0.01 & 0 \\ 0 & 0 & 0 & 0 & 0 & 0.01 \end{bmatrix},$$

$$R = 0.0001,$$

## 5.1 Simulations based on finite-horizon control model

Simulations of corrections against different timings perturbations in finite-horizon model are illustrated as figure 5.1, 5.2. Gray squares imply the velocity before perturbation onset, which we don't consider about, the three different curves implies three different timings. Against both kinds of perturbations, the finite-horizon model predicted time-dependent movement corrections.

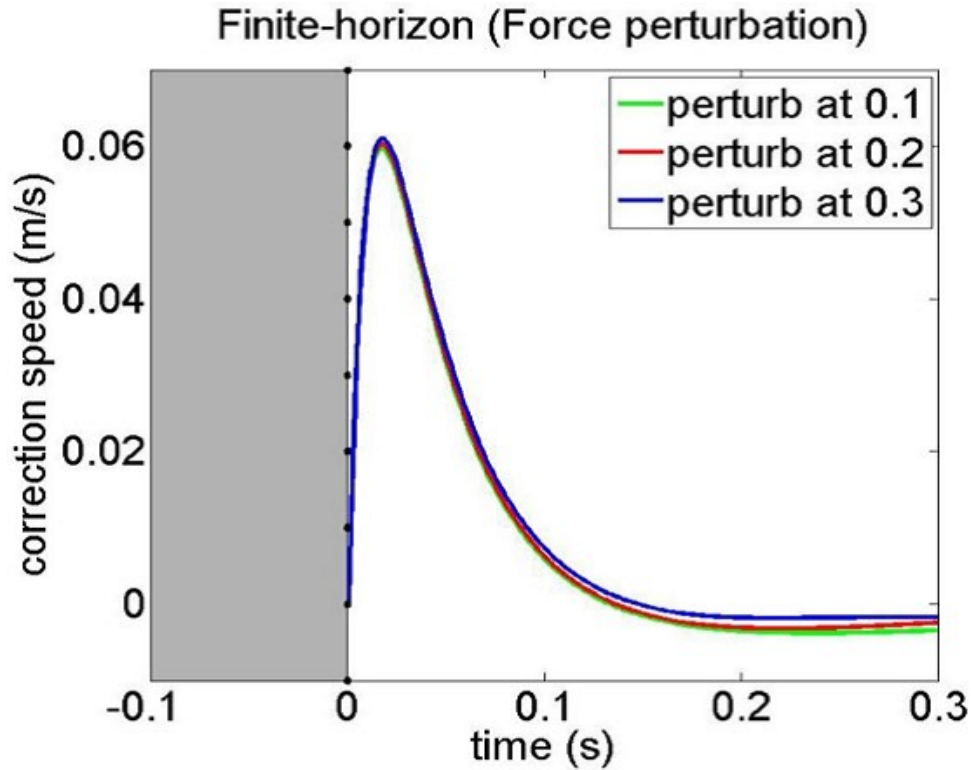


Figure 5.2: Force disturb corrections of finite horizon control

## 5.2 Simulations based on infinite-horizon control model

Simulations of corrections against different timings perturbations in infinite-horizon model are illustrated as figure 5.3, 5.4, three curves overlap under infinite-horizon control model in both visual and force conditions.

## 5.3 Sensory delay

To add the sensory delays, we model each perturbation as it occurring 120 ms later than the corresponding experimental perturbation in visual perturbation conditions according to [12], however, in force perturbation conditions, the mechanical push disturb the state immediately.

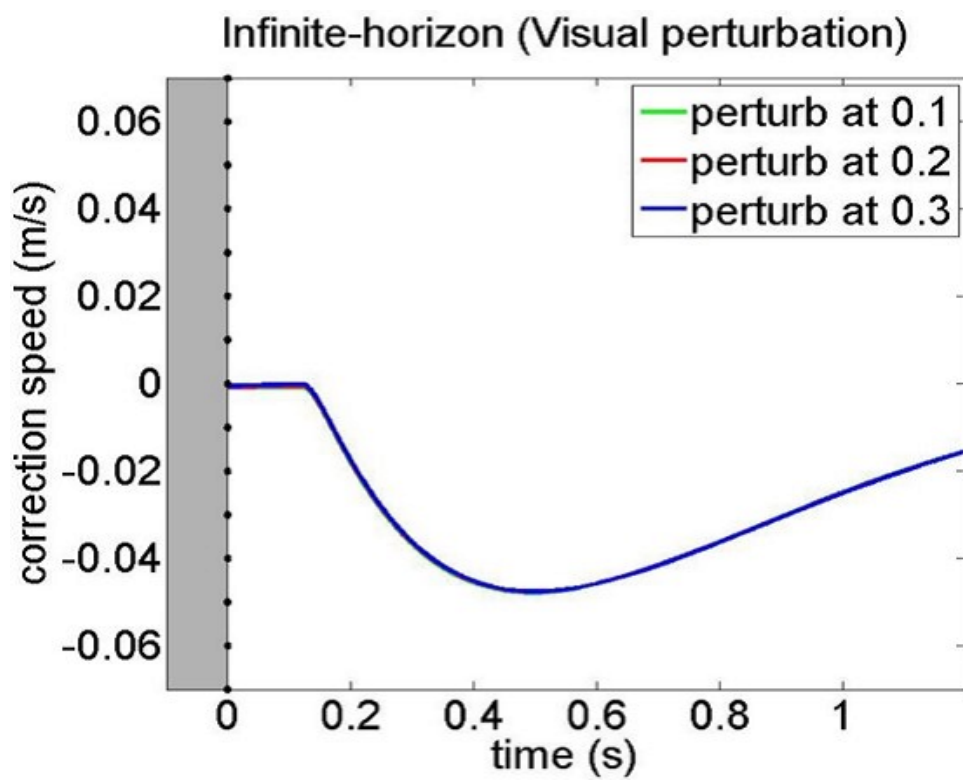


Figure 5.3: Visual disturb corrections of infinite horizon control

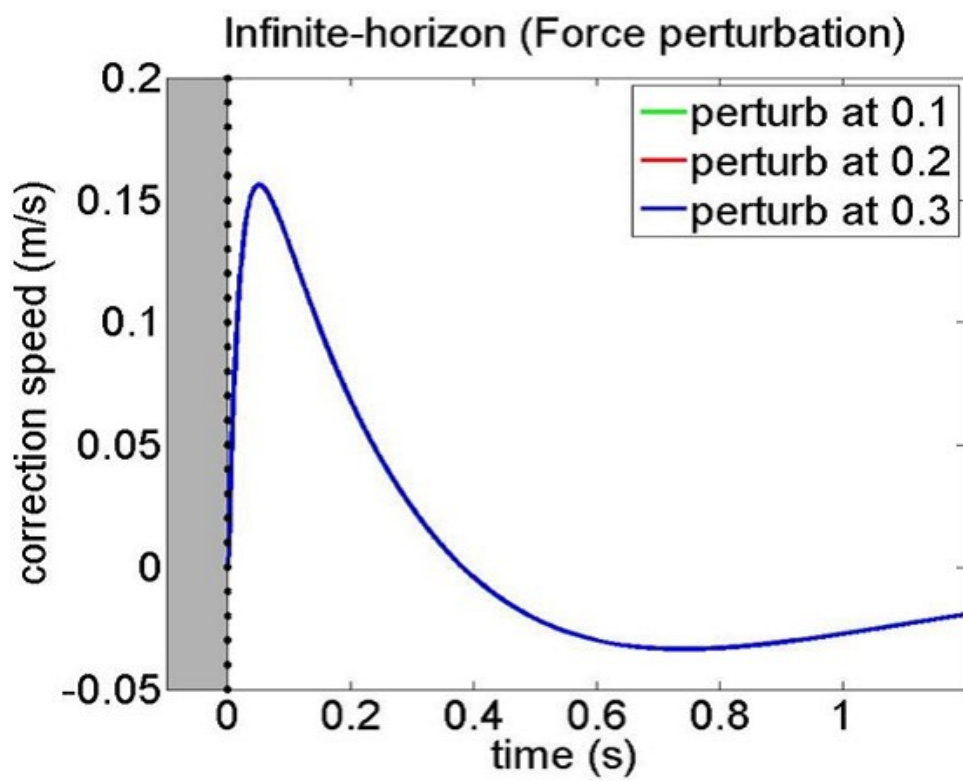


Figure 5.4: Force disturb corrections of infinite horizon control

# Chapter 6

## Data analysis

### 6.1 Whole data analysis

The experiment data of corrections against visual and force conditions are illustrated as figure 6.1, 6.2. We plot the mean values and the variances (error bar).

In visual condition, the blue curve is significantly different to the red and green curves, but the red and blue are highly overlap.

In force condition, these three curves overlap at the beginning and diverge later. The reason for the overlap at the beginning (the first peak velocity) is that the amplitude of force perturbation are same in each perturbation timing and the correction is not occurred immediately due to the sensory delay,

To make sense of the experiment result, We did statistical test at the peak value, in visual condition,  $F(2, 2295) = 39.55, P < 0.01$ ; in force condition,  $F(2, 2316) = 66.13, P < 0.01$  (the black arrows indicate the timing of velocities used for a statistical test), these result implies that the corrections against external perturbations of different timing are different. Moreover, the gains should be time-variant.

### 6.2 Separated data

Include the control trials, each subject performs 780 trials. During performing, they became familiar with the experiment trial by trial. Is it possible that the corrections are different at the beginning and become closer after learning? Is it possible that they use one control theory at the beginning and change to the another after getting familiar?

In order to answer this question, we separated the experiment data, which are shown as figure 6.3, 6.4. The left four figures are former trials of different directions, the right four are later trials.

Because they performed both forward and backward movements, and there is no guarantee for learning in one direction transferred to the opposite, so we also separated forward and backward movement, left perturbations and right perturbations. The figures shows that both in visual and force conditions, there are no significant between before and after learning.

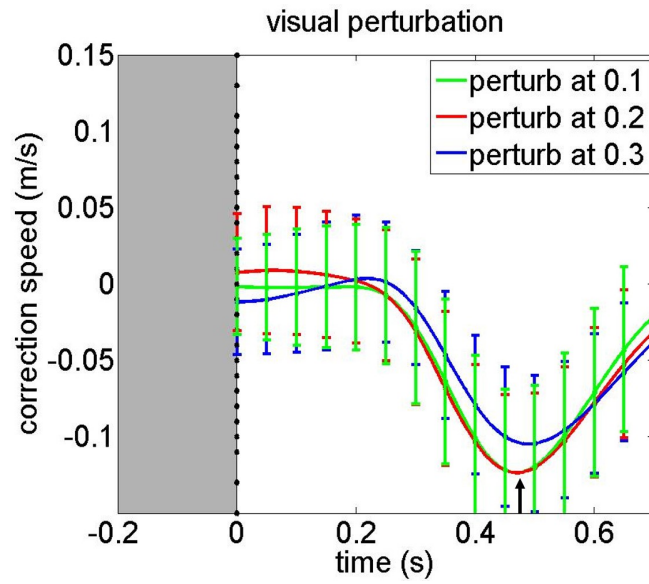


Figure 6.1: Corrections against visual perturbations

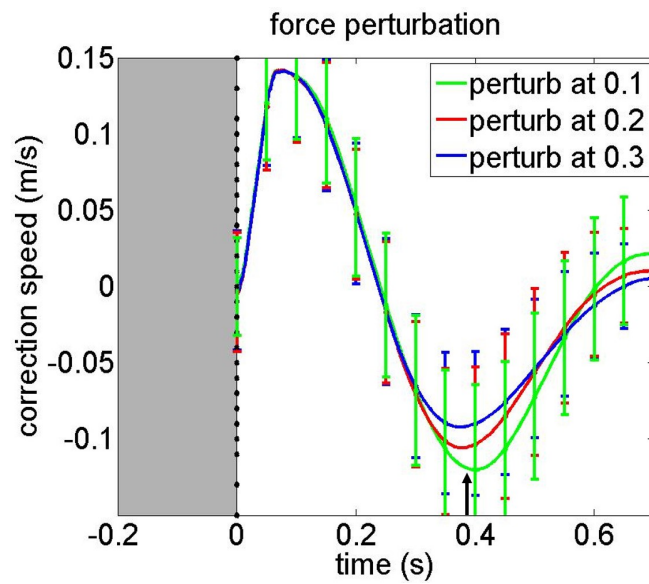


Figure 6.2: Corrections against force perturbations

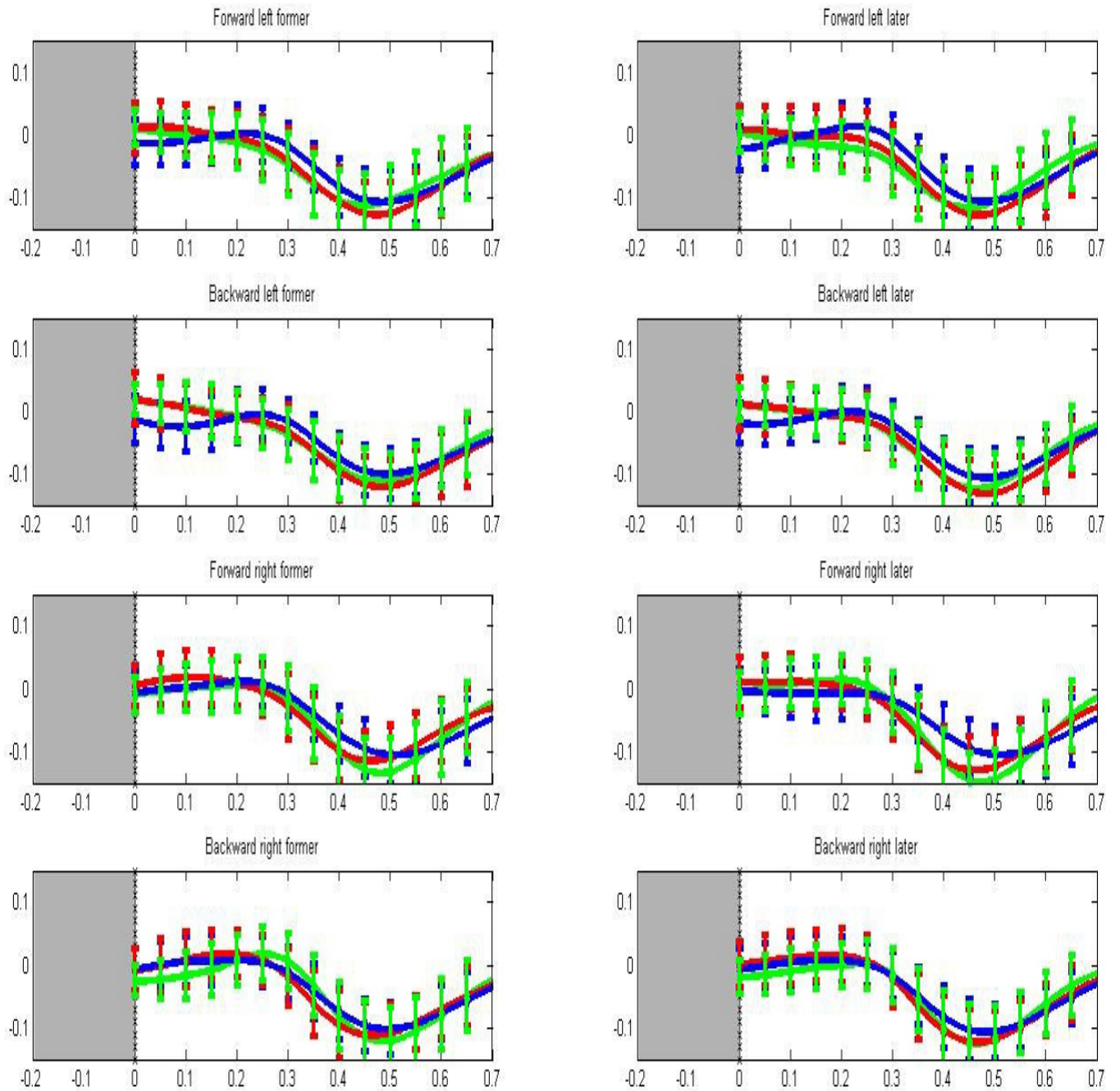


Figure 6.3: Separate data of visual condition

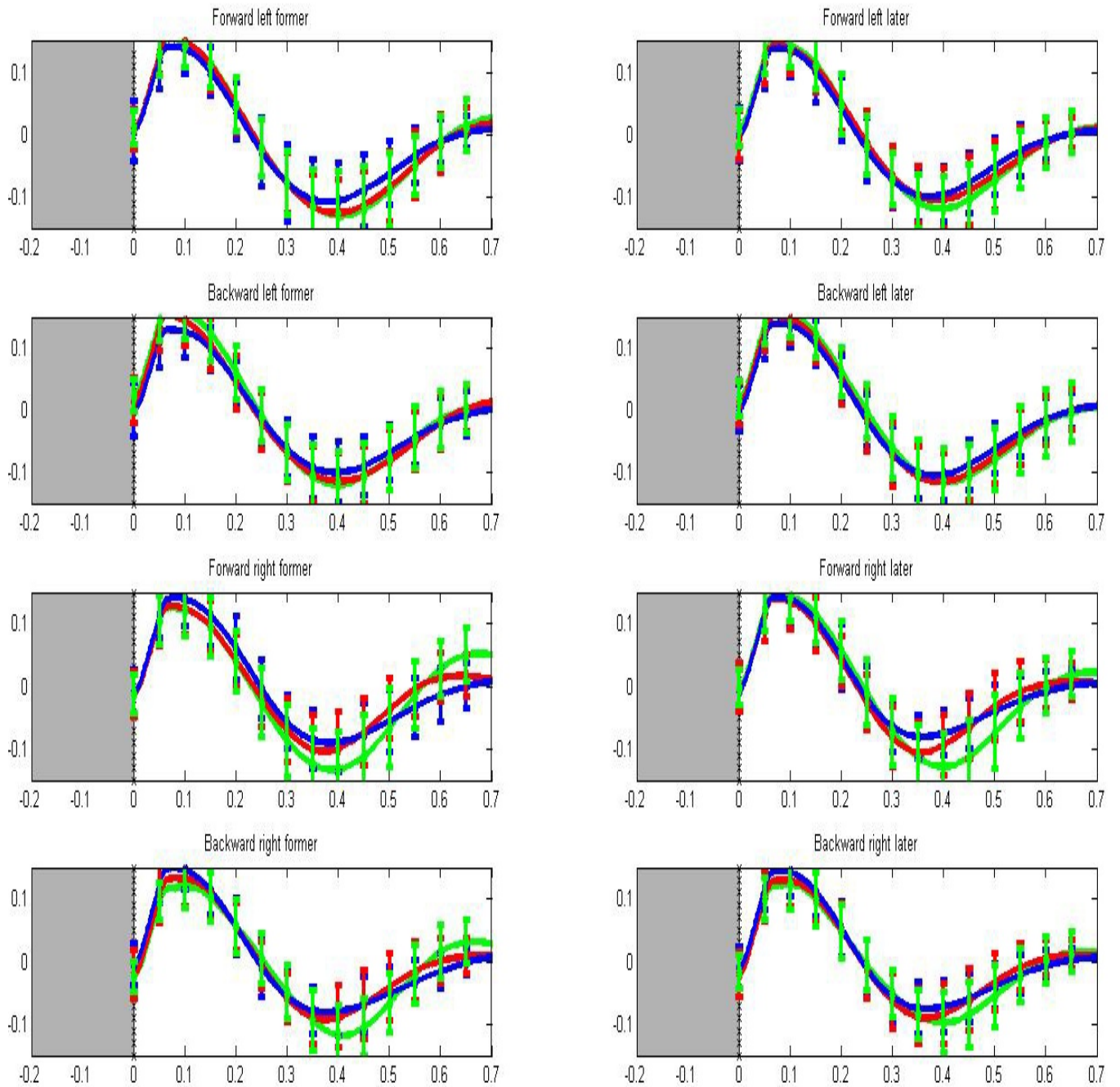


Figure 6.4: Separate data of force condition

The P values of both visual and force conditions are shown in table 6.1 6.2. In visual conditions, the p values of forward movement with left perturbations and backward movement with right perturbations become smaller, and the p values of forward movement with right perturbations and backward movement with left perturbations become larger. However, all of them are smaller than 0.05. In force conditions, there are almost no difference between former trials and later trials.

Table 6.1: Visual condition

	Former	Later
Forward left	0.16	1.77e-8
Forward right	0.0018	0.005
Backward left	3.86e-05	0.0103
Backward right	0.0187	8.28e-36

Table 6.2: Force condition

	Former	Later
Forward left	3.2e-71	7.7e-68
Forward right	1.7e-67	1.6e-72
Backward left	7.6e-64	1.1e-74
Backward right	4.0e-65	4.5e-72

# Chapter 7

## Tuning parameters

The experiment results indicates the gains are time-variant, so the infinite-horizon control model is inconsistent with our experiment data. Is finite-horizon control model totally consistent with experiment results? In the simulation of visual perturbation correction under finite-horizon control model, the order of the three curves are inconsistent with experiment data. In the framework of optimal feedback control, we optimize the movement by minimizing the cost. If we tune the cost matrixes, the order of the three curves could be changed. The  $Q, U, H$  matrices are expressed as

$$Q=U=H=\begin{bmatrix} w_{p_x} & 0 & 0 & 0 & 0 & 0 \\ 0 & w_{p_y} & 0 & 0 & 0 & 0 \\ 0 & 0 & w_{v_x} & 0 & 0 & 0 \\ 0 & 0 & 0 & w_{v_y} & 0 & 0 \\ 0 & 0 & 0 & 0 & w_{a_x} & 0 \\ 0 & 0 & 0 & 0 & 0 & w_{a_y} \end{bmatrix},$$

in the simulations above, and  $R$  is a scalar.

$w_{p_x}$  implies the weight brain assign on position error on  $x$  dimension, similarly  $w_{p_y}, w_{v_x}, w_{v_y}, w_{a_x}, w_{a_y}$  imply the weights brain assign on position error on  $y$  dimension, velocity errors on  $x$  and  $y$  dimension, acceleration errors on  $x$  and  $y$  dimension.

If the values we assign on different dimensions are quite different, it will induce jitter in trajectories, because two dimensions interact each other; if the difference of weights between two dimensions are so small, it does not change the order of the curves. Then we simply set  $w_{p_x} = w_{p_y}, w_{v_x} = w_{v_y}, w_{a_x} = w_{a_y}$ , and we use the parameters  $w_{p_x} = 1, w_{v_x} = 0.1, w_{a_x} = 0.01$  in previous chapter, it make sense if we change these values. For the motor cost  $R$ , force is motor command pass through a low-pass filter, and  $F = ma$ , so tuning  $R$  is almost no difference with tuning  $w_{a_x}$  and  $w_{a_y}$ .

Then we made a table contains

$$w_{p_x} = w_{p_y} = 0.01 * 2^n, n \in (1, 2, \dots, 10) \quad (7.1)$$

$$w_{v_x} = w_{v_y} = 0.001 * 2^n, n \in (1, 2, \dots, 10) \quad (7.2)$$

$$w_{a_x} = w_{a_y} = 0.0001 * 2^n, n \in (1, 2, \dots, 10) \quad (7.3)$$

to see if there is any tendency in this 1000(10<sup>3</sup>) unit database.

As shown in figure 7.1 7.2 . $V_1$  denotes the peak value of the correction velocity against early perturbations,  $V_2$  denotes the peak value of the correction velocity against middle perturbations,  $V_3$  denotes the peak value of the correction velocity against later perturbations. In most cases,  $V_1 < V_2 < V_3$ , with the decrease of weights we assign on velocity, the orders of  $V_1 < V_2 < V_3, V_2 < V_1 < V_3, V_2 < V_3 < V_1, V_3 < V_2 < V_1$  are also observed. there are totally six possible orders ( $V_1 < V_2 < V_3, V_1 < V_3 < V_2, V_2 < V_1 < V_3, V_2 < V_3 < V_1, V_3 < V_1 < V_2, V_3 < V_2 < V_1$ ), other two conditions are not occurred by applying this table.

In our experiment results of visual condition, the red curve and green curve are highly overlap, and are below the blue curve, which is nearly  $V_1 = V_2 < V_3$ , so we choose a group of value between  $V_1 < V_2 < V_3$  and  $V_2 < V_1 < V_3$  from figure 7.1 in order to fit the data. From figure 7.3, we notice that even though the order is consistent with the experiment data, the shape is very different. It is because the parameters we use here are:

$$Q=U=H= \begin{bmatrix} 0.45 & 0 & 0 & 0 & 0 & 0 \\ 0 & 0.45 & 0 & 0 & 0 & 0 \\ 0 & 0 & 0.01 & 0 & 0 & 0 \\ 0 & 0 & 0 & 0.01 & 0 & 0 \\ 0 & 0 & 0 & 0 & 0.25 & 0 \\ 0 & 0 & 0 & 0 & 0 & 0.25 \end{bmatrix},$$

The  $w_{v_x}$  and  $w_{v_y}$  are so small and  $w_{a_x}$  and  $w_{a_y}$  are large, which means they don't care much about the velocity accuracy but care about the acceleration. The "correction" we defined is the velocity in perturbation dimension, and the acceleration is the derivative of the velocity. So this case implies: after the positional errors are corrected, they don't stop the hand, because they care more acceleration than velocity.

In our simulations, we set  $Q = U = H$  in order to simplify the computation. If we ignore the time complexity, we should remove this constrain. In that case, the size of the database become 1000000000(1000<sup>3</sup>), which takes so long time to compute.

In the simulations, we simply assumed that the cost on each steps are equal, but they could be different. We can't experience all the different weights.

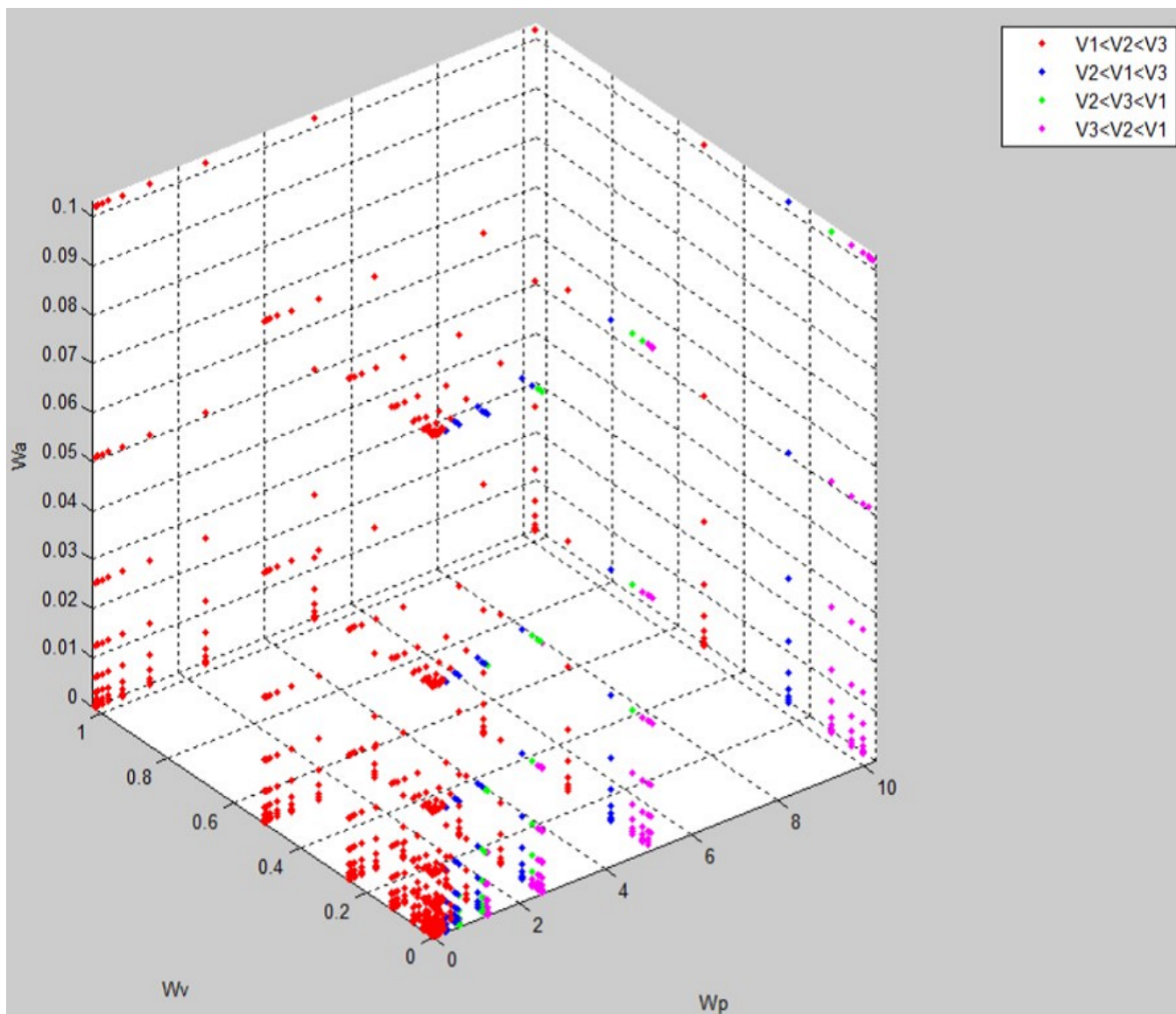


Figure 7.1: Orders in visual condition

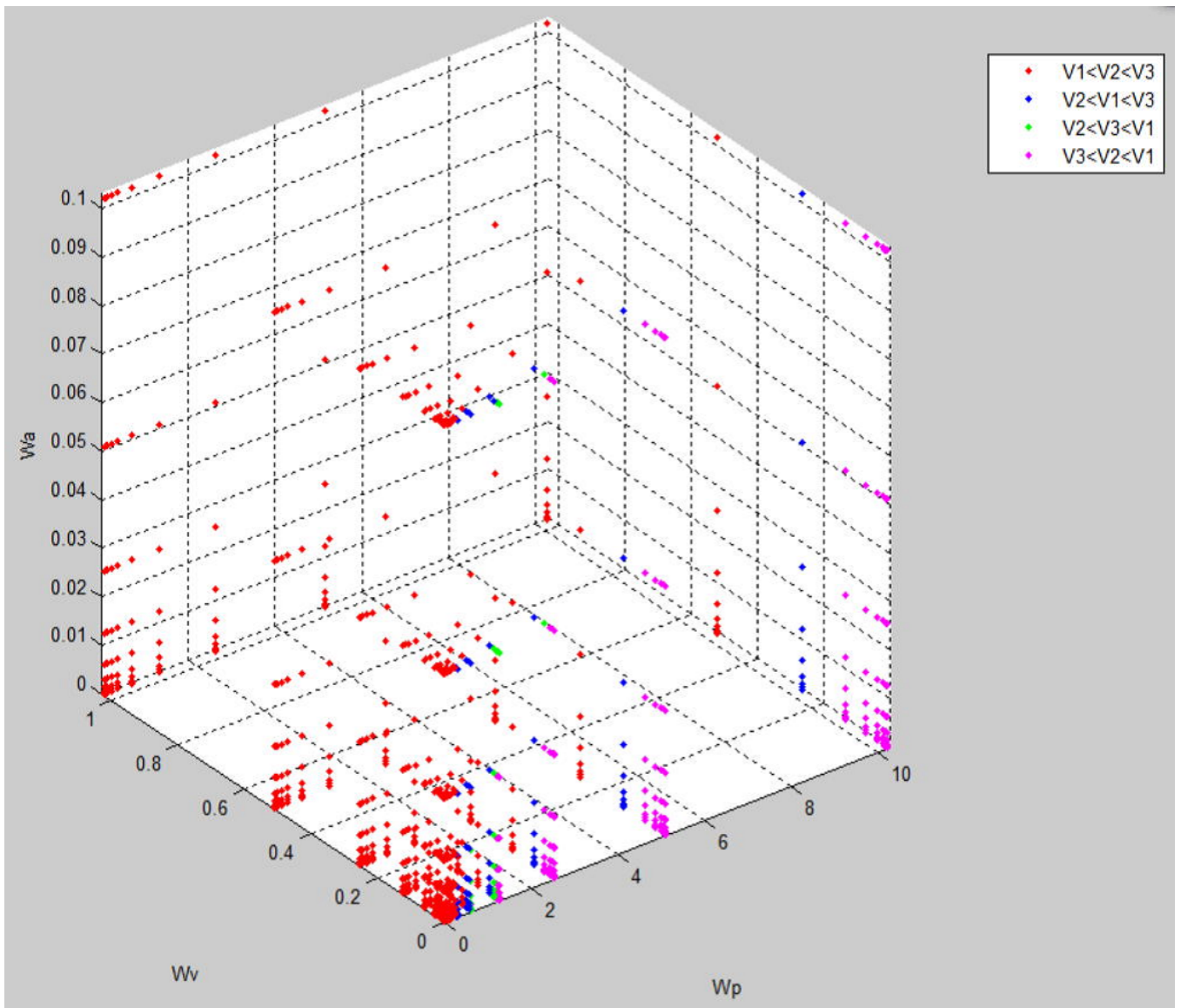


Figure 7.2: Orders in force condition

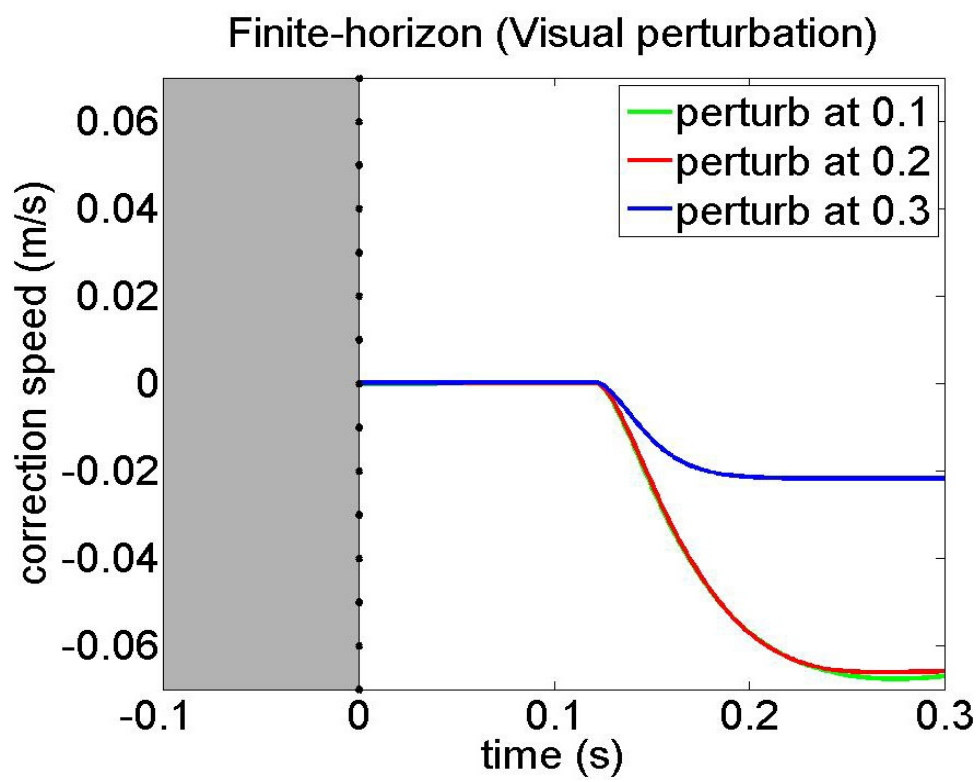


Figure 7.3: tune

# Chapter 8

## Conclusion

### 8.1 Summary

The velocity values were statistically different in the visual and force-perturbation conditions even though the early and middle perturbation corrections of visual condition are highly overlap.

There is no significant difference between former trials and later trials in each conditions from both curve shapes and statistical tests.

To fit the experiment data via finite-horizon control, none of the weight in our database(1000) is appropriate. Neither can we go-over all the possible weights.

### 8.2 Discussion

Some of the experiment results are consistent with finite-horizon control, but the results can not totally explained by finite-horizon model in our simulations. The optimal feedback control has so many degrees of freedom, we can not go over every possibilities.

### 8.3 Conclusion

This study addressed a question of whether the brain predetermines a movement duration and made a detailed analysis regarding the predictions of finite- and infinite-horizon optimal feedback control models in an experimentally testable way. We reported the result of reaching experiment with visual or force perturbations.

We found the method to investigate whether movement duration is known before onset by comparing finite-horizon model and infinite-horizon model. We compared these two model by checking whether the gains are time-variant or time-invariant. We designed target reaching task with perturbations to check the gains by measuring whether corrections against different timings are different or same.

We found that the experiment results is inconsistent with infinite-horizon control. In order to fit the experiment data, we tuned the parameters in finite-horizon control. Un-

fortunately, none of the weight in our database(1000) is able to fit the experiment data. Further research may consider how to find the tendency of the curves (correction) in order to explain the data.

The results indicated that the movement duration is not emerged after finishing the movement, but whether it is definitely determined before onset is still an open question.

## 8.4 Acknowledgement

I would like to appreciate my supervisor of this project, Associate Professor Hirokazu Tanaka for the great helps and advices. He provided me this idea and gave me much economy support. I would like to thank Professor Jianwu Dang, Assistant Professor Atsuo Suemitsu and Assistant Professor Shinichi Kawamoto who give me a lot of good suggestions. I would like to thank Professor Hiroshi Imamizu and Mr. Yoshioka who support my experiment. I would like to thank Professor Hajime Asama who gave me good advices during my poster session. Also, I would like to thank every one in Tanaka lab and Dang lab who have given helps to me.

# Bibliography

- [1] Tanaka, H., Krakauer, J. W., and Qian, N. (2006). An optimization principle for determining movement duration. *Journal of Neurophysiology*, 95, 3875-3886.
- [2] Harris, C. M., and Wolpert, D. M. (2006). The main sequence of saccades optimizes speed-accuracy trade-off. *Biological Cybernetics*, 95, 21-29.
- [3] Shadmehr, R., de Xivry, J. J. O., Xu-Wilson, M., and Shih, T.Y. (2010). Temporal discounting of reward and the cost of time in motor control. *The Journal of Neuroscience*, 30, 10507-10516.
- [4] Todorov E. (2005). Stochastic optimal control and estimation methods adapted to the noise characteristics of the sensorimotor system. *Neural computation*, 17, 1084-1108.
- [5] Qian, N., Jiang, Y., Jiang, Z. P., and Mazzoni, P. (2013). Movement duration, fitts's law, and an infinite-horizon optimal feedback control model for biological motor systems. *Neural Computation*, 25, 697-724.
- [6] Shadmehr R., and Mussa-Ivaldi S. (2012) *Biological learning and control: how the brain builds representations, predicts events, and makes decisions*. Mit Press.
- [7] Fitts, Paul M. (1954). The information capacity of the human motor system in controlling the amplitude of movement. *Journal of Experimental Psychology* 47 (6): 381C391.
- [8] Phillis, Y. A. (1985). Controller design of systems with multiplicative noise. *Automatic Control, IEEE Transactions on*, 30, 1017-1019.
- [9] Oldfield R C. (1971) The assessment and analysis of handedness: the Edinburgh inventory. *Neuropsychologia*, 9(1): 97-113.
- [10] Winter, D. (1990). *Biomechanics and motor control of human movement*. New York: Wiley.
- [11] Yu J, Zhong-Ping J, Ning Q. (2011) Optimal control mechanisms in human arm reaching movements. *Control Conference (CCC), 30th Chinese. IEEE*, 2011: 1377-1382.

- [12] Liu D, Todorov E. (2007) Evidence for the flexible sensorimotor strategies predicted by optimal feedback control. *The Journal of Neuroscience*, 27(35): 9354-9368.
- [13] Todorov E, Jordan M I. (2002) Optimal feedback control as a theory of motor coordination. *Nature neuroscience*, 5(11): 1226-1235.